INFLUENCE OF FABRICATION CONDITIONS ON MICROSTRUCTURAL AND OPTICAL PROPERTIES OF LEAD-FREE FERROELECTRIC $Bi_{0.5}Na_{0.5}TiO_3$ MATERIALS

LE THI HAI THANH[†], NGUYEN HOANG TUAN, LUONG HUU BAC,
AND DANG DUC DUNG

School of Engineering Physics, Hanoi University of Science and Technology

PHUNG QUOC BAO

Faculty of Physics, College of Science, Vietnam National University, Hanoi

[†]*E-mail:* haithanh0609@gmail.com

Abstract. *Lead-free ferroelectric materials have attracted considerable attention due to the increasing potential applications in environmentaly benign materials. Among lead-free ferroelectric materials, the $Bi_{0.5}Na_{0.5}TiO_3$ (BNT) materials have been paying more attention because they exhibit good ferroelectric and piezoelectric properties, making BNT materials become promising candidates to replace $Pb(Zr,Ti)O_3$. In this work, the lead-free ferroelectric BNT materials were synthesized by sol-gel method. The effect of fabrication parameters on microstructural and optical properties was studied. These parameters include Na precursor concentration and calcination temperature. The results indicated that the Na precursor concentration higher 40 mol.% and calcining at temperatures in the region of 800-1000°C for 2h in air were the best conditions to synthesize lead-free BNT materials.*

Keywords: lead-free, $Bi_{0.5}Na_{0.5}TiO_3$, optical properties, sol-gel.

Classification numbers: 42.70.Mp; 81.20.Fw; 78.67.Bf.

I. INTRODUTION

Lead-free ferroelectric materials have attracted considerable attention due to increasing potential applications in environmentaly benign materials. The reason is that in the past decade the traditional ferroelectric materials, $Pb(Zr,Ti)O_3$ (PZT), which contain a large amount of lead (~ 60 wt.%), have caused environmental concerns, as well as inconsistent with governmental regulations

against hazardous substances [1]. Among lead-free ferroelectric materials, the $Bi_{0.5}Na_{0.5}TiO_3$-based (BNT) materials are intensively studied in the hope of replacing the lead containing PZT-based materials [2]. As useful materials for the piezoelectric and ferroelectric applications, the lead-free ferroelectric BNT materials are also promising for environment treatments due to their high photocatalytic activity. Ai *et al.* reported that BNT materials displayed superior activity for photocatalytic removal of gaseous nitric oxide over TiO_2 under simulated sunlight irradiation [3]. In addition, the super photocatalytic water-splitting capability of BNT for H_2 evolution has been reported [4]. Moreover, Li *et al.* reported that BNT showed photocatalytic activity in the photo-degradation of methyl orange [5]. The ferroelectric materials are good candidates for photocatalytic applications because they exhibited natural spontaneous polarization that results in reduce the recombination time of electron-hole pair, which is generated from photon energy [6]. The ferroelectric materials displayed the large lifetime of electron-hole pair around ms which was 10^6 times larger than that of TiO_2 (around ns) [6, 7].

The BNT materials, which have been fabricated by traditional solid state method, were widely investigated. This method requires a long manufacturing time and uses a lot of energy. Hence, a simple method with low sintering temperature, short sintering time and relatively inexpensive feedstock is required for the preparation of BNT ceramics. The sol-gel method is an effective and low cost method for synthesis of ceramics. However, the loss of Na element during synthesis affects dramatically on stoichiometry of synthesized BNT ceramics and subsequently it will impact strongly on the ferroelectric and optical properties, as well as photocatalytic activity [8, 9]. In this aspect, *A*-site nonstoichiometry that could occur at any step of the process will cause intrinsic defects [8]. Therefore, the study the influence of fabrication conditions on structural and optical properties of lead-free BNT materials are essential to achieve the high-quality BNT-based lead-free piezoelectric ceramics.

In this work, the lead-free ferroelectric BNT materials were synthesized by sol-gel method. The effects of fabrication parameters including gel-process and calcination temperature on microstructural and optical properties were systematically studied. The results indicated that the Na precursor concentration over 40 mol.% of stoichiometric Na-site cations and the calcination temperature in the region of 800-1000°C for 2h in air were the best conditions to obtain pure lead-free BNT materials.

II. EXPERIMENT

The lead-free ferroelectric BNT samples were synthesized by the sol-gel method. The raw materials are bismuth nitrate pentahydrate ($Bi(NO_3)_2.5H_2O$), sodium nitrate ($NaNO_3$), and tetraisopropoxytitanium (IV) ($C_{12}H_{28}O_4Ti$). The acetic acid (CH_3COOH) and acetylacetone ($CH_3COCH_2COCH_3$) were selected as solvents. The fabrication procedure for the lead-free ferroelectric BNT was as follows. Firstly, bismuth nitrate pentahydrate and sodium nitrate were dissolved in acetic acid and distilled water. After vigorously stirred for 1 h, a transparent homogeneous sol was formed. Then, the acetylacetone and the tetraisopropoxytitanium (IV) were introduced into the transparent solution. The solution was continuously stirred until the solution changed to light yellow color. The solution was dried at 100 °C to get gel. The sodium concentration varied from 0 to 50 mol% of stoichiometric Na-site cations to investigate its evaporation to stoichiometry of BNT materials. The dry gels were ground and calcined at 400 °C for 2 h and sintered at various temperature from 500 to 1000 °C for 3 h. After sintering, the white BNT

powder was obtained The powder morphology was studied using a field emission scanning electron microscope (FE-SEM). The crystalline structures of the samples were characterized by X-ray diffraction (XRD). The optical properties were studied by UV-VIS spectroscopy.

III. RESULTS AND DISCUSSION

Figure 1 shows the X-ray diffraction patterns of lead-free BNT samples sintered at 800˚C for 3h in air with various Na concentration in region of 0-50 mol% of stoichiometric Na-site cation. The results indicated that the sintered materials were single phase with rhombohedral structure when the Na concentration was over 40 mol%. These X-ray diffraction patterns are in agreement with those reported in the previous works [10, 11]. The pyrochlore $Bi_2Ti_2O_7$ and some other unidentified impurity phases were formed when the Na concentration is less than 40 mol%. The pyrochlore $Bi_2Ti_2O_7$ phase also appeared during fabrication of BNT thin films by sol-gel method [12].
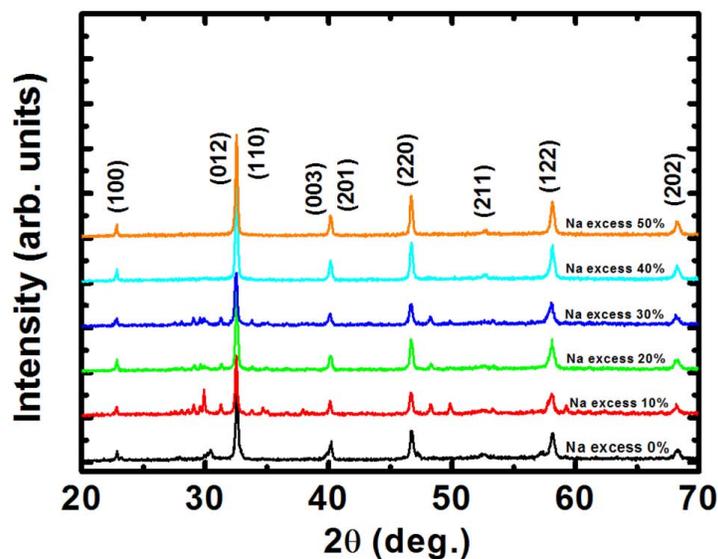
Fig. 1. X-ray diffraction patterns of BNT samples calcined at 800˚C for different Na precursor concentration.

Based on the results of XRD analysis, we chose the 50 mol% Na precursor concentration to investigate the effect of calcination temperature on the phase structure. Figure 2 shows the influence of calcination temperature on phase structure of $Bi_{0.5}Na_{0.5}TiO_3$. The XRD patterns indicated that the impurity phases appeared when the calcination temperature was smaller than 800˚C . The single phase BNT samples with perovskite structure was obtained at calcination temperatures higher than 800˚C . The result also showed that the BNT phase was formed and stable at temperatures higher than 800˚C. It can be seen that the best conditions to synthesize the BNT ceramics using sol-gel method are the Na precursor concentration in the range of 40-50 mol.% and the calcination temperature of 800-1000˚C .
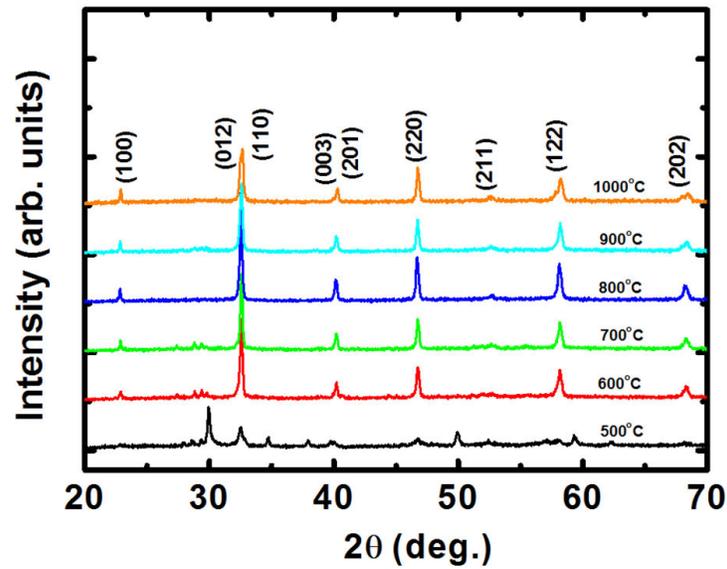
Fig. 2. X-ray diffraction patterns of BNT samples calcined at different temperatures with Na precursor concentration of 50 mol%.
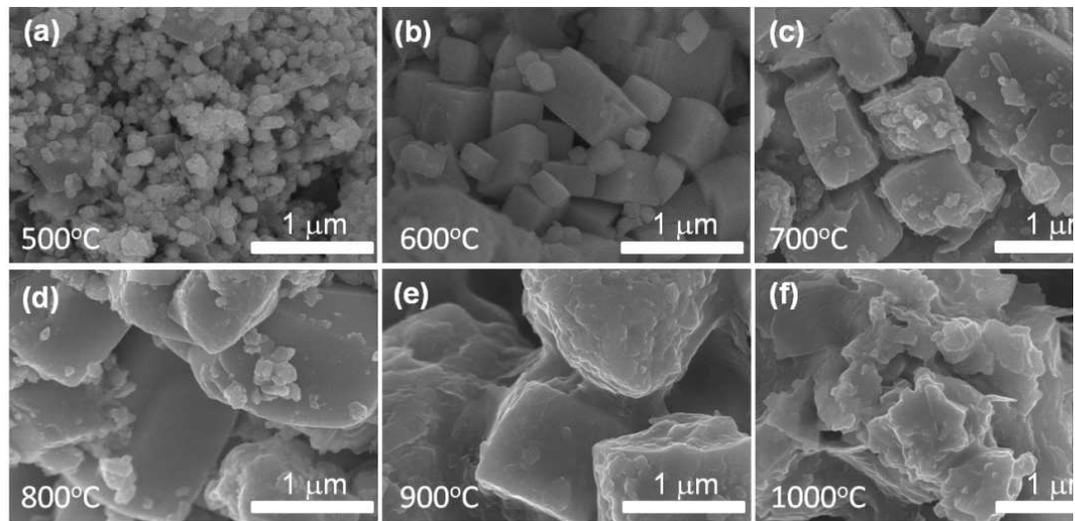
Fig. 3. FE-SEM images of BNT samples calcined at different temperatures: (a) 500˚C , (b) 600˚C , (c) 700˚C , (d) 800˚C , (e) 900˚C and (f) 1000˚C.

Figure 3 shows the surface morphology of BNT samples which have been calcined at various temperature from 500-1000˚C . The results showed that the grain size increased with calcination temperature. At calcination temperature of 500˚C, the grains were small and round in shape.

The grains became bigger at calcination temperature of 600˚C. It is interesting that the grain shape becomes cubic at this calcination temperature. Besides cube-like shape, the small irregular shape particles appeared at calcination temperature of 700 and 800˚C. At calcination temperature higher than 900˚C, the particles were sintered and conglomerations were formed.

Figure 4 shows the optical absorption spectra of samples calcined at different temperatures. The result clearly indicated that the absorption band is strongly dependent on the calcination temperature. The sample calcined at 500˚C exhibited one absorbance band with a small tail (Fig. 4 a). However, two small tails appeared when the sample was calcined at 600˚C (Fig. 4b). The optical absorption spectra for samples calcined at 700˚C exhibited the overlap of two absorbance bands as shown in Fig. 4(c). We suggested that the secondary phase might contribute to the optical absorption spectra of BNT samples. The single absorbance band was obtained for samples calcined at 800 and 900˚C, as shown in Fig. 4(d) and Fig. 4(e), respectively. The results are consistent with the single BNT phase structure as indexed from XRD patterns. By increasing the calcination temperature up to 1000˚C , the absorbance tail appeared again in the optical absorption spectrum which might be the result of nonstoichiometry of BNT and/or contribution of oxygen vacancies during calcination at high temperature.
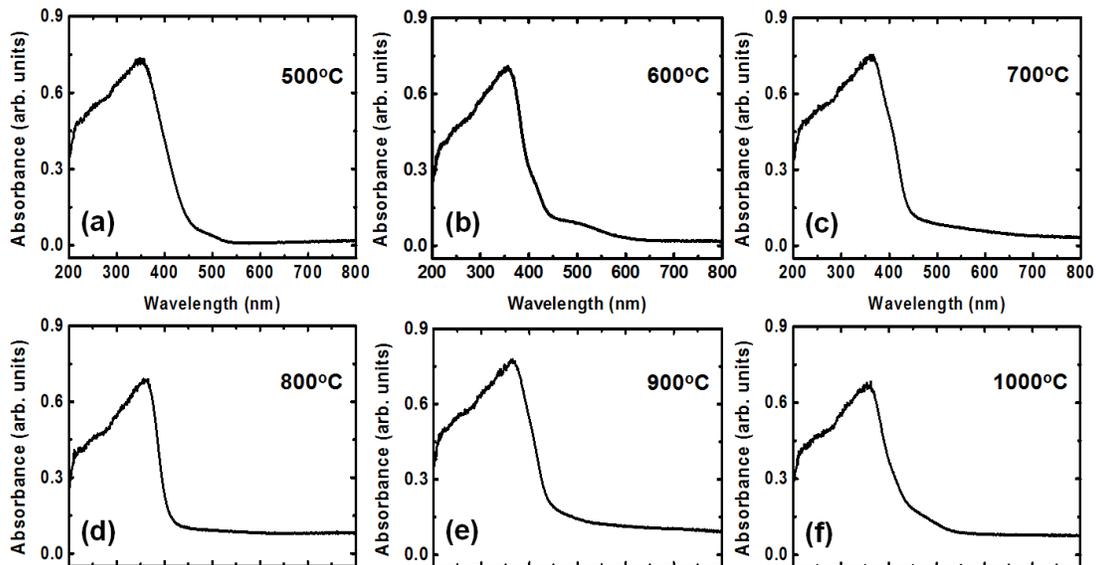
Fig. 4. UV–Vis absorption spectra of BNT calcined at different temperatures.

The optical bandgap energy (E_g) was estimated by the method proposed by Wood and Tauc [13]. According to this method, the optical bandgap is associated with the absorbance and photon energy by the following equation: $\alpha h \nu = c(h\nu - E_g)^n$, where α is the absorbance coefficient, h - the Planck constant, ν - the frequency, E_g - the optical bandgap and n - a constant associated with different types of electronic transition ($n = 1/2, 2, 3/2$ or 3 for direct allowed,

indirect allowed, direct forbidden and indirect forbidden transitions, respectively) [13]. The optical bandgap E_g can be obtained from the intercept of $(\alpha h\nu)^{1/n}$ versus photon energy $h\nu$. The bandgap values estimated with $n = 1/2$ for direct transition for calcination temperatures from 500-1000 °C (Fig. 5) varied from 3.00 eV to 3.14 eV which were slightly dependent on the calcination temperature.
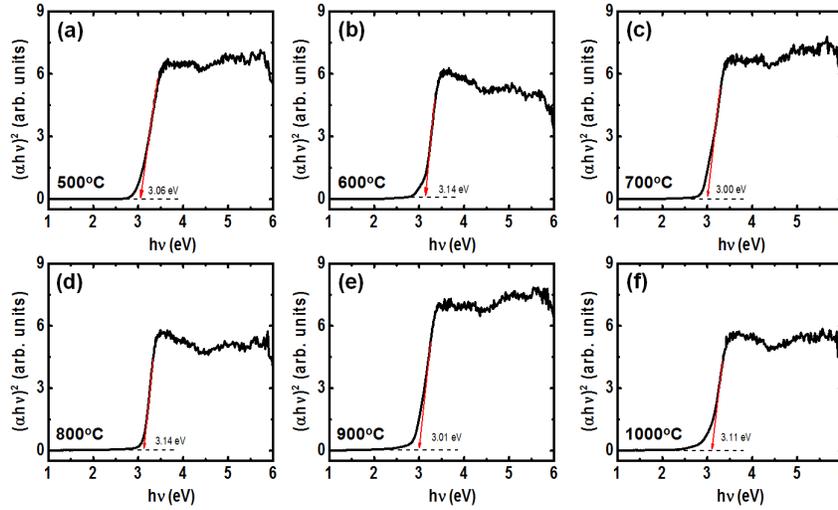
Fig. 5. Plots of $(\alpha h\nu)^2$ versus $h\nu$ for BNT samples calcined at different temperatures for direct transition.
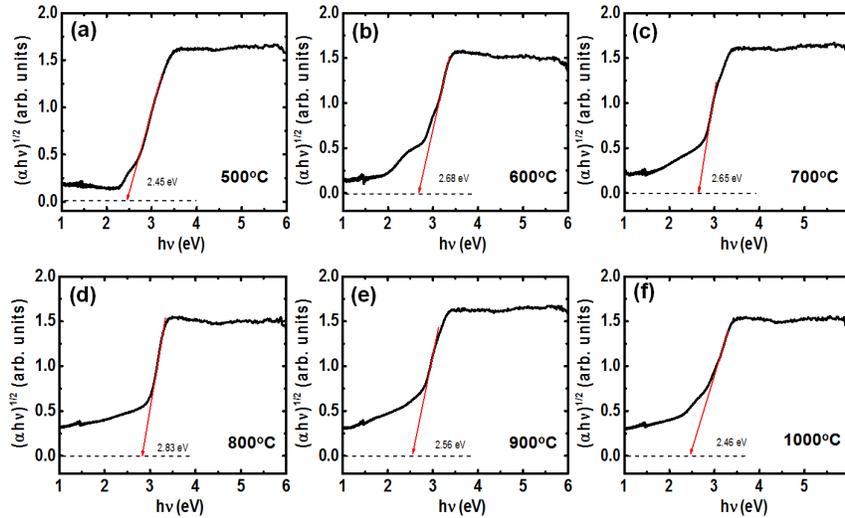
Fig. 6. Plots of $(\alpha h\nu)^{1/2}$ versus $h\nu$ for BNT samples calcined at different temperatures for indirect transition.

Furthermore, the bandgap values have been estimated with $n = 2$ for indirect transition for calcination temperature from 500-1000˚C (Fig. 6) These values varied from 2.45 eV to 2.83 eV with slight dependence on the calcination temperature as in the case of direct transition. However, the bandgap values were smaller than those of the case of direct transition. These trends are consistent with published reports [14, 15]. Kim *et al.* obtained the BNT bandgap energy of 3.5 eV for direct transition and 3.0 eV for indirect transition [14], which are similar to those of $Bi_4Ti_3O_{12}$ [16]. In the case of $BaTiO_3$, the photon bandgap energy is 3.3 eV for indirect transition and 4.0 eV for direct transition [15].

IV. CONCLUSION

The effects of Na precursor concentration and calcination temperatures on microstructural and optical properties of BNT materials have been investigated. The BNT single phase was obtained for Na precursor concentration higher than 40 mol.% of stoichiometric Na-site cation and the calcination temperature in the range of 800-1000˚C . The optical band gap was slightly dependent on the calcination temperature and changed from 3.00 to 3.14 eV for direct transition and from 2.45 to 2.83 eV for indirect transition.

ACKNOWLEDGEMENT

REFERENCES

[1] E. Cross, *Nature* **432** (2004) 24–25.

[2] N. D. Quan, L. Huu Bac, D. V. Thiet, V. N. Hung, and D. D. Dung, *Advances in Materials Science and Engineering* **2014** (2014) .

[3] Z. Ai, G. Lu, and S. Lee, *Journal of Alloys and Compounds* **613** (2014) 260–266.

[4] L. Wang and W. Wang, *Int J Hydrogen Energy* **37** (2012) 3041–3047.

[5] J. Li, G. Wang, H. Wang, C. Tang, Y. Wang, C. Liang, W. Cai, and L. Zhang, *Journal of Materials Chemistry* **19** (15) (2009) 2253–2258.

[6] Y. Lin, C.-W. Nan, J. Wang, H. He, J. Zhai, and L. Jiang, *Materials Letters* **58** (5) (2004) 829–832.

[7] X. Yang, Z. Dai, A. Miura, and N. Tamai, *Chemical Physics Letters* **334** (4) (2001) 257–264.

[8] Y. S. Sung and M. H. Kim, *Nonstoichiometry in $(Bi_{0.5}Na_{0.5}) TiO_3$ ceramics*, Lead-Free Piezoelectrics, Springer, 2012, pp. 353–370.

[9] I.-K. Jeong, Y. Sung, T. Song, M.-H. Kim, and A. Llobet, *Journal of the Korean Physical Society* **67** (9) (2015) 1583–1587.

[10] H. Nagata and T. Takenaka, *Journal of the European Ceramic Society* **21** (10) (2001) 1299–1302.

[11] A. Watcharapasorn, S. Jiansirisomboon, and T. Tunkasiri, *Materials Letters* **61** (14) (2007) 2986–2989.

[12] D. H. Kang and Y. H. Kang, *Journal of the Microelectronics and Packaging Society* **20** (4) (2013) 25–30.

[13] D. Wood and J. Tauc, *Physical Review B* **5** (8) (1972) 3144.

[14] C.-Y. Kim, T. Sekino, and K. Niihara, *Journal of Sol-gel Science and Technology* **55** (3) (2010) 306–310.

[15] H. Matsuda, N. Kobayashi, T. Kobayashi, K. Miyazawa, and M. Kuwabara, *Journal of Non-crystalline Solids* **271** (1) (2000) 162–166.

[16] H. Gu, D. Bao, S. Wang, D. Gao, A. Kuang, and X. Li, *Thin Solid Films* **283** (1) (1996) 81–83.